

Errata in my book "Electrical machines and drives"

(some changes may have been applied already in the final type-set version of the book; here, I referred to the first version)

Chapter 3, page 95

Now we consider a multiphase (armature) winding. An m-phase (distributed) winding normally contains $2m$ phase belts in a double pole pitch. In Fig. 3.9, (a) and (b) show schematically the winding configurations of a three-phase armature with $2m = 6$ phase belts and $q = 3$, for four and two poles respectively. In (c) in Fig. 3.9, a linear representation of a double pole pitch (2π electrical radians) is depicted.

Chapter 3, page 108

This voltage can also be interpreted as a transformer voltage, where $\hat{\Psi} = (w \cdot \xi) \cdot \hat{\Phi}$ is the amplitude of the alternating flux coupled with the armature winding. Here, the winding factor takes into account that for a distributed winding the axes of the q coils are not all aligned with the flux axis. The alternating flux coupled with them is then lower by the cosine of the inclination angle.

If the winding axis is inclined over an angle γ with respect to the flux axis, see (b) in Fig. 3.15, the induced voltage of Eq. 3.57 (or the coupled flux) must be multiplied by $\cos \gamma$.

....

The factor ν in the denominator stems from the flux calculation where $\nu - 1$ half pulses annihilate (ν is always odd). We remark that the already small field harmonics from a distributed winding (reduced by $\xi_\nu^*/\nu \approx 1/\nu^2$ for large q , where ξ_ν^* is the winding factor of the field winding) are again reduced by a factor $\xi_\nu/\nu \approx 1/\nu^2$. Thus the total reduction is about $(1/\nu)^4$. For large q (in both field winding and armature), the emf harmonics are therefore negligible.

Chapter 3, page 111

An actual slot winding with a finite number of slots may, for the fundamental flux, also be treated as an air-gap winding. Indeed, we have (with ξ_1 the actual winding factor for finite q)

$$\hat{A}_1 = \frac{m}{2} \cdot \frac{(2w\xi_1) \cdot \hat{I}_f}{N_p \tau_p} = \frac{(2w\xi_1) \cdot \hat{I}_f}{2N_p(\tau_p/m)}$$

....

In the previous sections we have seen that a symmetrical multiphase current in a symmetrical multiphase winding generates a rotating field. Further, we derived that a symmetrical emf is induced in a symmetrical multiphase winding when it is located in a rotating magnetic field. Note that current and voltage (emf) occurring at the same time in the same winding will (or rather may) correspond to electrical power.

In this section we will analyse the torque that will (or may) come into being when a current carrying (symmetrical multiphase) winding is located in a (rotating) magnetic field. This torque will (or may) give rise to mechanical **power**.

Chapter 4, page 124

On the other hand, a symmetrical m_2 -phase secondary current $i_2(t) = \hat{I}_2 \cos \omega_1 t$ results in a rotating field (with $x' = 0$ along the secondary axis):

$$b_2(x', t) = \hat{B}_2 \cos(\omega_1 t - \frac{x' \pi}{\tau_p}) = \hat{B}_2 \cos(\omega_1 t - \frac{x \pi}{\tau_p} + \alpha) \quad (4.37)$$

as $x' = x - \alpha \tau_p / \pi$.

Chapter 4, page 128

Thus the resulting torque exerted by the field on the rotor will try to rotate the rotor in the direction of the field. If the rotor is free to rotate, the rotor will try to reach synchronism with the field. Finally, at synchronous speed, $\Omega_m = \Omega_{sy} = \omega_1 / N_p$, the induced emf in the rotor, the rotor current and the torque will become zero.

Chapter 4, page 133

In a similar way as for a transformer, simplified equivalent circuits can be derived. However, there are some differences as the magnetising inductance of an induction machine is (relatively) much smaller while the leakage reactances are much higher, see **the table 4.1**.

Chapter 4, page 135

Equation 4.87 shows that the primary (stator) electromagnetic power is transferred *by the rotating field* partly into **mechanical power** $P_m = T \Omega_m$ and partly by transformer action into electrical power in the rotor, the secondary (rotor) electromagnetic power P_{em2} . For a short-circuited rotor this secondary electromagnetic power is equal to the joule losses in the rotor resistance, $P_{em2} = m_2 E_2 I_2 \cos \psi_2 = m_2 R_2 I_2^2 = m_1 R_2' I_2'^2$. If an external circuit or power source (with slip frequency) is connected to the slip rings the secondary electrical power is partly (P_2) transferred to this circuit or power source (and partly into rotor joule losses).

Chapter 4, page 137

To derive the expression for \underline{I}'_2 we use the Thévenin equivalent circuit as observed from the rotor, Fig. 4.10 (which can be derived from Fig. 4.8, omitting the iron loss resistance, or from Fig. 4.6 by reversing the sign of \underline{I}_2):

$$\underline{I}'_2 = \frac{\underline{V}'_{2o}}{R'_{k2} + jX'_{k2}} \quad (4.90)$$

with

$$\underline{V}'_{2o} = \underline{V}_1 \frac{jX_{m1}}{R_1 + jX_{1\sigma} + jX_{m1}} \approx \frac{\underline{V}_1}{1 + \sigma_1} \quad (4.91)$$

$$\underline{Z}'_{k2} = R'_{k2} + jX'_{k2} \approx \left[\frac{R_1}{(1 + \sigma_1)^2} + R'_2/s \right] + j \left[X'_{2\sigma} + \frac{X_{1\sigma}}{1 + \sigma_1} \right] \quad (4.92)$$

where the primary leakage coefficient is defined by $\sigma_1 = X_{1\sigma}/X_{m1}$, and with $\left[X'_{2\sigma} + \frac{X_{1\sigma}}{1 + \sigma_1} \right] = \sigma X'_2 \equiv X'_{\sigma 2}$ the total leakage as observed from the secondary.

This results in

$$T \simeq \frac{m_1}{\Omega_{sy}} \left[\frac{\underline{V}_1}{1 + \sigma_1} \right]^2 \frac{R'_2/s}{\left[\frac{R_1}{(1 + \sigma_1)^2} + R'_2/s \right]^2 + \left[X'_{2\sigma} + \frac{X_{1\sigma}}{1 + \sigma_1} \right]^2} \quad (4.93)$$

If the stator resistance can be neglected, this simplifies to

$$T \simeq \frac{m_1}{\Omega_{sy}} \left[\frac{\underline{V}_1}{1 + \sigma_1} \right]^2 \frac{R'_2/s}{[R'_2/s]^2 + X'^2_{\sigma 2}} \quad (4.94)$$

For small slip values ($s \ll R'_2/X'_{\sigma 2}$), on the one hand, equation 4.94 can be approximated to

$$T \simeq \frac{m_1}{\Omega_{sy}} \left[\frac{\underline{V}_1}{1 + \sigma_1} \right]^2 \frac{s}{R'_2} \quad (4.95)$$

i.e. the torque varies about linearly with s .

For large values of the slip ($s \gg R'_2/X'_{\sigma 2}$), on the other hand, the torque varies hyperbolically with the slip:

$$T \simeq \frac{m_1}{\Omega_{sy}} \left[\frac{\underline{V}_1}{1 + \sigma_1} \right]^2 \frac{R'_2/s}{X'^2_{\sigma 2}} \quad (4.96)$$

In between the torque reaches a maximum value, the pull-out (or breakdown) torque:

$$T_{po} \simeq \pm \frac{m_1}{\Omega_{sy}} \left[\frac{\underline{V}_1}{1 + \sigma_1} \right]^2 \frac{1}{2X'_{\sigma 2}} \quad (4.97)$$

The corresponding slip value is called the pull-out slip:

$$s_{po} = \pm R'_2/X'_{\sigma 2} \quad (4.98)$$

Chapter 4, page 161

As depicted in Fig. 4.34 the flux $\underline{\phi}_{mc} = L_{mc}(\underline{I}_c + \underline{I}'_e)$ lags the flux $\underline{\phi}_{me} = L_{me}\underline{I}_e$ by an angle α . But the symmetry axes of the fluxes $\underline{\phi}_{mc}$ and $\underline{\phi}_{me}$ (thus the axes of the parts δe and $(1 - \delta)e$ of the pole) are also shifted in space, by

an angle β . By decomposing both alternating fields into two equal and counter-rotating fields we obtain a situation as depicted in Fig. 4.35. The left rotating fields may almost completely annihilate each other while the right rotating fields add up. The result is a large right rotating field and a small relic of the left rotating field. A pure rotating field requires $\phi_{mc} = \phi_{me}$, $\alpha + \beta = \pi$ and $\alpha = \beta$ or thus $\alpha = \beta = \pi/2$. Although a time shift of 90° is quite feasible, a space shift of 90° is physically impossible (as this would boil down to a magnetic short-circuit of adjacent north and south poles).

Chapter 5, page 187

Suppose $M(V, i_f)$ is a point on this load characteristic for an inductive current I (Fig. 5.19). Then the corresponding point $N(E_r, i_m)$ will be on the no-load characteristic. The vertical distance between N and M is equal to $X_\sigma I$, while the horizontal distance between these two points is equal to αI . Both points are therefore connected by a rectangular triangle¹⁴ with all sides proportional to I . For a constant I , this triangle remains congruent while point N stays on the no-load characteristic. Thus the load characteristic for this constant I is found by shifting the no-load characteristic in the direction of the vector \underline{NM} .

Chapter 5, page 189

The load characteristic for a pure capacitive load is therefore found by shifting the no-load characteristic upwards in the direction of the vector \underline{NM}^* (see Fig. 5.22).

Chapter 5, page 192

These control characteristics can be derived graphically¹⁸ starting from the load characteristics.

5.2.8.4 External characteristics

The external characteristics show the relation between voltage and armature current for a given excitation current and a given $\cos \varphi$. These characteristics also illustrate the magnetising effect of capacitive loads versus the demagnetising effect of inductive loads.

These external characteristics can also be derived graphically¹⁹ starting from the load characteristics (Fig. 5.26).

¹⁴ This triangle is called the Potier triangle; for a given machine (X_σ and α) these triangles are always similar; the triangle is also called the short-circuit triangle, see the triangle ABC .

¹⁸ In the load characteristics, draw a horizontal line corresponding to the given terminal voltage. Consider then the Potier triangles with point N on the no-load characteristic and the sides PM (or QM) on this horizontal line.

¹⁹ In the load characteristics, draw a vertical line corresponding to the given excitation current. Consider then the Potier triangles with point N on the no-load characteristic and the sides PN on this vertical line.

Chapter 5, page 202-203

Projection of these current components on the real and imaginary axes then yields the real (or active) and imaginary (or reactive) current components

$$I_{re} = I \cos \varphi = \frac{E_p \sin \beta}{X_d} + \frac{1}{2} V \left(\frac{1}{X_q} - \frac{1}{X_d} \right) \sin 2\beta \quad (5.57)$$

$$I_{im} = -I \sin \varphi = \left[-\frac{E_p \cos \beta}{X_d} + V \left(\frac{\sin^2 \beta}{X_q} + \frac{\cos^2 \beta}{X_d} \right) \right] \quad (5.58)$$

The expressions for torque, active and reactive power are therefore

$$T = \frac{3}{\Omega} \left(\frac{V E_p \sin \beta}{X_d} + \frac{1}{2} V^2 \left(\frac{1}{X_q} - \frac{1}{X_d} \right) \sin 2\beta \right) \quad (5.59)$$

$$P = 3 \left(\frac{V E_p \sin \beta}{X_d} + \frac{1}{2} V^2 \left(\frac{1}{X_q} - \frac{1}{X_d} \right) \sin 2\beta \right) \quad (5.60)$$

$$Q = 3 \left(\frac{V E_p \cos \beta}{X_d} - V^2 \left(\frac{\sin^2 \beta}{X_q} + \frac{\cos^2 \beta}{X_d} \right) \right) \quad (5.61)$$

Chapter 5, page 207

But synchronous machines are also frequently used as a motor and, although in terms of total energy converted this might seem less important, in terms of the number of applications (and machines) this may **outreach by far** the number of synchronous generators.

Chapter 6, page 214

Note that a thyristor may come into conduction in other abnormal ways (in addition to an anode-to-cathode voltage exceeding the forward **break-over voltage**):

- by a very high dV_A/dt , resulting in a capacitive ignition
- when, after a conduction interval, the positive anode-to-cathode voltage returns too quickly.

Chapter 6, page 219

The three terminals are called collector, emitter and base. In power electronic applications, the transistor is normally used as a switch by providing sufficient base current if it is switched on. When the basis current I_B is zero, the BJT essentially behaves as an open circuit, with high high collector-emitter voltage V_{CE} and low collector current I_C . For a sufficiently high basis current, the transistor enters saturation and approximately behaves as a closed switch with a

relatively low voltage drop (see the characteristics $I_C - V_{CE}$ in (c) in Fig. 6.9 or the characteristics $V_{CE} - I_B$ in (d) in Fig. 6.9).

A transistor is current-controlled: the basis current determines the open or closed condition. To keep the collector-emitter voltage sufficiently low, the basis current must be high enough; for high collector currents, the gain I_C/I_B may become less than 10. A much higher gain (100 or more) can be obtained using a Darlington pair, as is illustrated in (e) in Fig. 6.9.

Chapter 7, page 251

Therefore, defining $S_o = V_{do} \cdot I_d$, we may write the expressions for active, reactive and apparent power as follows:

Chapter 8, page 264

The switch Th must be able to switch on and off (e.g. a GTO or IGBT or IGCT or Mosfet). During interval T_1 , the source delivers current to the load (Th conducting). When Th is switched off at $t = T_1$, the current continues flowing through the diode as the load is inductive. The load voltage is then zero. At $t = T_1 + T_2$ the switch is turned on again, and so on periodically with period $T = T_1 + T_2$. Assuming a steady-state condition, the following equations are valid in the intervals $0 \leq t \leq T_1$ and $T_1 \leq t \leq T_1 + T_2$:

Chapter 8, page 265

From Eqs. 8.5 and 8.6, I_M and I_m can be calculated. In most cases, $T \ll \tau$. Using $\exp(-x) \approx 1 - x$, we can approximate I_m and I_M by

$$I_m \approx \alpha I_1 + \beta I_2 - \alpha \beta \frac{T}{\tau} I_1 \quad (8.7)$$

$$I_M \approx \alpha I_1 + \beta I_2 - \alpha \beta \frac{T}{\tau} I_2 \quad (8.8)$$

where $\alpha = T_1/T$ and $\beta = 1 - \alpha = T_2/T$.

Chapter 10, page 294-296

However, the output voltage will contain much larger harmonics of lower order (e.g. 3, 5, 7,...)³. Fig. 10.11 compares the output waveforms for voltage and current of sinusoidal and trapezoidal modulation. It is clear that the output current is much more distorted for the trapezoidal modulation.

Note that this figure also is interesting as it shows which converter operates at each instant, as well as the rectifying or regenerating (inverter) operation.

³ For three-phase systems triple harmonics do not harm; then a trapezoidal waveform with limited fifth harmonic will be chosen

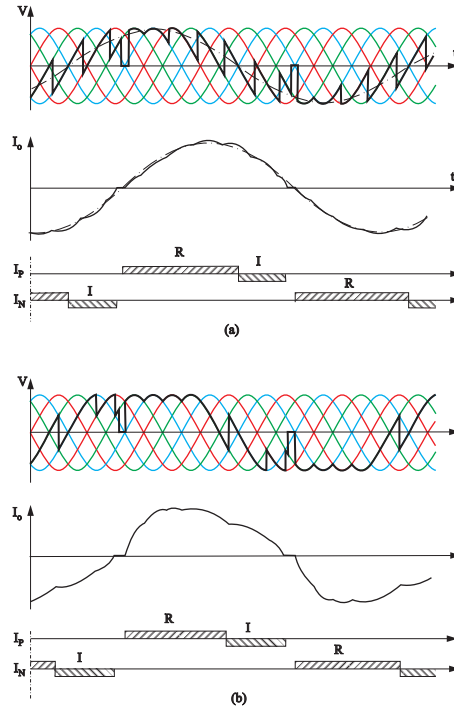


Fig. 10.11 Trapezoidal modulation versus sinusoidal modulation

Chapter 10, page 301

Which harmonics occur in the output voltage depends on whether a circulating current is present and, if no circulating current is present, on the load power factor. In case of a free circulating current, the output voltage is the average of the positive and negative converter voltages: $v_o = (v_p + v_n)/2$. As has been illustrated in 10.13, the output voltage is much smoother. Indeed, many harmonics are cancelled out. Of the harmonics in equations 10.2 and 10.3, only a limited number remain in the output, as now the **inequalities $2l \leq 3(2k - 1) + 1$ and $2l + 1 \leq 6k + 1$** apply to the families f_{h1} and f_{h2} , respectively.

Chapter 11, page 313

Curve (d) in Fig. 11.8 illustrates the DC link current for an inductive load. In interval I, only switch T_1 is conducting at the plus side of the source, and the current i_d in the DC link therefore equals **the (then lagging) AC current** in phase U. In the other intervals as well, the current i_d follows the current in the corresponding phase and thus the shape of the current i_d is a repetition of this sine-wave segment. Note that in each interval, first the anti-parallel diode is conducting and the switch takes over when the current reverses sign (on condition that the gate signal for the switch is still present). Commutation to the next interval requires the switch to be turned off explicitly so that the diode of the opposite switch takes over (e.g. D_2 from T_2' from interval I to II). If the switch were not turned off explicitly, the DC source would short circuit.

Curve (e) in Fig. 11.8 illustrates the DC link current for a capacitive load. In interval I, only switch T_1 is conducting at the plus side of the source and thus the current i_d in the DC link equals **the (then leading) AC current** in phase U. Similarly, in the other intervals, the current i_d follows the current in the corresponding phases and again we obtain the shape of the current i_d as a repetition of this sine-wave segment. Note that now, in each interval, first the switch is conducting and the anti-parallel diode takes over when the current reverses sign. For the commutation to the next interval, switching on the opposite switch should, in principle, be sufficient to cause the current to commute to this side (e.g. T_2 from D_2' from interval I to II). However, an explicit turn-off signal will always be given to the previous

switch (T_2 in this example) before turning on the next one (T_2'), because otherwise a short circuit of the DC source would ensue if the load was not (or not sufficiently) leading.

Chapter 11, page 322

The principle for obtaining PWM in three-phase inverters is basically the same as for single-phase inverters. The reference waves for the three phases are displaced by 120° and thus the output fundamental will consist of symmetrical three-phase sinusoids. Similar conclusions as for the single-phase inverter hold true for the three-phase inverter:

- the output fundamental amplitude is proportional to the amplitude of the reference wave if the amplitude modulation index m_a is less than 1
- if the frequency modulation index m_f is large enough, pure harmonics of the fundamental will be absent.

Chapter 13, page 365-366

The equivalence between DC and AC current amplitudes can be derived from Fig. 13.9: to the left, (a), we see the DC situation and to the right, (c), we see the instantaneous condition in AC at the instant the current in phase U is zero (time axis as in (b)). Thus, if the DC current I_{DC} is equal to $(\sqrt{3}/2)\hat{I}$, then its mmf is the same as the mmf $(3/2)\hat{I}$ of a three-phase current \hat{I} , which means that also the torques are equivalent. In other words, a DC current I_{DC} has the same effect as an AC current kI_n (with I_n the effective value) if $I_{DC} = (\sqrt{3}/2) \cdot kI_n$.

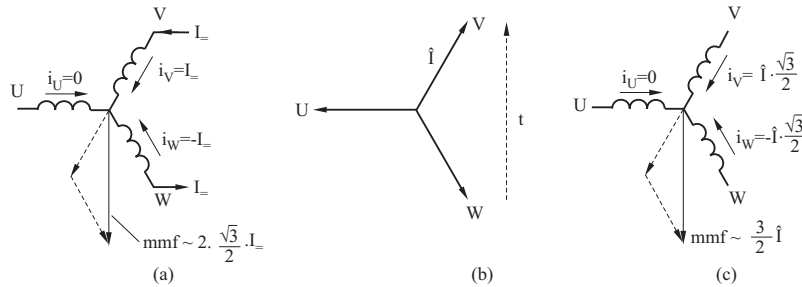


Fig. 13.9 Equivalence of DC and AC for the mmf

Chapter 13, page 378

Another standard scheme is the Scherbius cascade (see (a) in Fig. 13.24). The DC machine is mechanically connected to another induction machine, working as an over-synchronous generator. The secondary power is thus converted into electrical power. Although the DC machine is now operated at high speeds and lower current, this scheme requires three electrical machines. Moreover, this secondary power is not directly converted into mechanical energy for the load. On the other hand, low-speed operation ($s_o > 0.5$) is possible. Speed control is also achieved by varying the excitation of the DC machine (in the diagram (b) in Fig. 13.23, the E_g lines are now horizontal lines).

Chapter 20, page 496

If the minor loop (or recoil line) for the operating point (H_{pm}, B_{pm}) can be linearised as (see Fig. 20.1)

$$B_{pm} = \mu_m(H_r + H_{pm}) = B'_r + \mu_m H_{pm} \quad (20.10)$$

Jan A. Melkebeek, May 24, 2018

<http://www.springer.com/978-3-319-72729-5>

Electrical Machines and Drives

Fundamentals and Advanced Modelling

Melkebeek, J.

2018, XXIX, 734 p. 575 illus., 91 illus. in color.,

Hardcover

ISBN: 978-3-319-72729-5